Journal of Materials Chemistry A

Accepted Manuscript

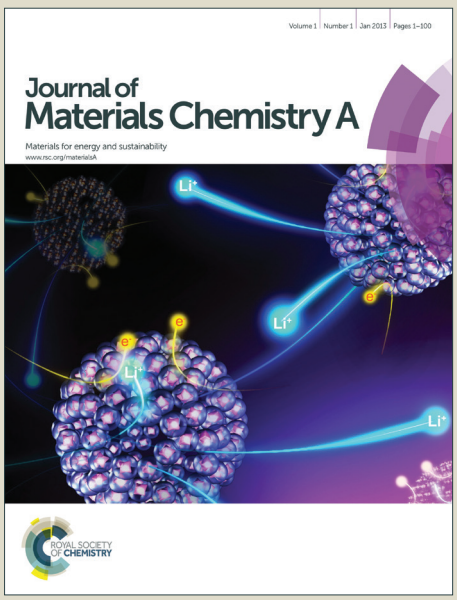

ROYAL SOCIETY OF CHEMISTRY

www.rsc.org/materialsA

Journal Name

RSCPublishing

ARTICLE

Regeneration of Sodium Alanate studied by powder *in situ* neutron and synchrotron X-ray diffraction†

Cite this: DOI: 10.1039/xoxxoooooox

Terry D. Humphries,[a] Joshua W. Makepeace,[b,c] Satoshi Hino,[a] William I. F. David[b,c] and Bjørn C. Hauback,[a]*

Received ooth January 2012,
Accepted ooth January 2012

DOI: 10.1039/xoxxoooooox

www.rsc.org/

The regeneration pathway of sodium alanate has been studied in detail by *in situ* synchrotron powder X-ray diffraction (SR-XRD) and powder neutron diffraction (PND). Rietveld refinement of the data has accurately determined the composition of all crystalline phases during the reaction process and shows definitively that Al initially reacts with NaH to form Na_3AlH_6, followed by the formation of $NaAlH_4$ (before the total consumption of NaH) in two indiscrete reactions. During hydrogenation, an expansion of 0.6 % of the Na_3AlH_6 unit cell is observed indicating towards the inclusion of Ti within the crystal lattice. This study promotes the recent development of next-generation sample holders and detectors that now enable the *in situ* diffraction measurement of hydrogen storage materials under relatively high gas pressures (>100 bar) and temperatures.

Introduction

Since the beginning of the industrial revolution, man-kind has become completely dependent on fossil fuels for heat, transport and the manufacture of everyday essentials. Although we are fully conscious of the imminent depletion of these fuels, we recognise the fact that we are not able to continue modern living without them. As such, the research and development of renewable energy supplies, alternative fuels and energy storage methods has become part of the international political and scientific discourse. Many possibilities for sustainable energy storage have been proposed, with electrochemical battery and hydrogen storage materials generally recognised to be the most viable long-term replacements for fossil fuels.

Sodium alanate ($NaAlH_4$) has arguably become the leading model for complex metal hydride-based hydrogen storage materials since the pioneering work by Bogdanović and Schwickardi.[1] The demonstration that the addition of selected titanium compounds to $NaAlH_4$ results in enhanced kinetics of reversible hydrogen storage under moderate conditions in the solid state has instigated a host of publications regarding the optimised cycling of this material (employing a variety of additives),[2-13] the mechanism involved in the reversible hydrogenation processes[14-29] and the adaption of the method to other complex metal hydrides.[30-34] The factor that has inhibited the commercialisation of $NaAlH_4$ for automobile applications is the unfavourable theoretical hydrogen capacity of 5.6 wt. %,[35] but the incorporation of this material into composites containing materials with higher hydrogen capacity has recently gained much attention.[36-38] $NaAlH_4$ destabilises metal hydrides, such as MgH_2, by modifying the thermodynamics and kinetics of the hydrogen sorption reaction.[36] The onset of decomposition is determined to occur at 280 °C, rather than 330 °C by the formation of $NaMgH_3$.

The decomposition pathway of $NaAlH_4$ (with and without additives) has been determined to occur in two discrete steps by a number of *in situ* powder X-ray diffraction (PXD),[16, 39] TEM,[25, 40] and NMR spectroscopy[41] studies. The first step is the decomposition of $NaAlH_4$ to Na_3AlH_6 releasing ~3.8 wt. % H_2, followed by the decomposition of Na_3AlH_6 to NaH releasing a further 1.8 wt. % H_2 (Eq. 1 and 2).[42] It has been determined that with the incorporation of Ti-additives, dehydrogenation occurs via the same reaction pathway despite the dramatic lowering of the activation energy for both of the dehydrogenation reactions.[1, 21] The role of the Ti additive has been under scrutiny and it is understood that after cycling, a zero valent Ti species is formed which remains unchanged after 100 cycles.[43] The Ti is understood to be atomically dispersed throughout the Al phase forming a variety of Al-Ti alloys.[15, 22, 43-47]

$$NaAlH_4 \rightleftarrows {}^1/_3Na_3AlH_6 + {}^2/_3Al + H_2 \quad (1)$$

$$Na_3AlH_6 \rightleftarrows 3NaH + Al + {}^3/_2H_2 \quad (2)$$

It has long been assumed that the rehydrogenation of NaH and Ti-enhanced Al (Al*) proceeds through the reverse of the two-step dehydrogenation process (Eqs. 1 and 2), entailing the complete conversion of NaH to Na_3AlH_6 before there is any significant formation of $NaAlH_4$. However, a recent *in situ* NMR spectroscopy experiment studying the regeneration of NaH/Al* with 140 bar H_2 indicated that a significant amount of

Na_3AlH_6 was formed within the first two minutes of H_2 addition and the onset of $NaAlH_4$ formation occurs after only four minutes.[20]

The design of next-generation detectors, and sample cells allowing the addition of at least 100 bar of gas pressure during experiments, now permits *in situ* regeneration of hydrogen storage materials to be conducted with good data statistics. In this study, the regeneration of $TiCl_3$-enhanced sodium alanate has been conducted *in situ* by SR-PXD and PND for the first time. These diffraction techniques facilitate the detection and quantification of all crystalline phases observed during the hydrogenation process. They enable a great contrast to NMR spectroscopy, which only allows for the observation of one nuclei and where quantification is problematic.[20] The correlation between the results obtained here using SR-PXD and PND, with those obtained by NMR spectroscopy allows for the definitive identification of the mechanism for the regeneration of $TiCl_3$-enhanced sodium alanate.

Experimental Details

$NaAlH_4$ was purchased from Albemarle Corporation (Lot No.: 22470404-01, >93% purity). $TiCl_3$ was purchased from Sigma-Aldrich Chemicals Inc. (99.995% purity). Deuterium gas was purchased from Yara AS (99.8 % purity). The powders were manipulated inside MBraun Unilab glove boxes filled with purified Argon (<1 ppm O_2, H_2O) to avoid contamination.

The NaH/Al with $TiCl_3$ additive starting material (NaH/Al*) was produced by the mechano-milling of $NaAlH_4$ with 2 mol% $TiCl_3$ using a Fritsch P6 planetary mill and a Fritsch GTM/II stainless steel vial and stainless steel balls. A ball to powder mass ratio of 20:1 was employed, with a milling time of 3 h, at a speed of 350 rpm. The resultant powder was then heated at 150 °C, *in vacuo* for 24 h.

The NaD/Al with $TiCl_3$ additive starting material (NaD/Al*) was produced by milling $NaAlH_4$ with 2 mol% $TiCl_3$ under the same conditions as the NaH/Al* powder. The resultant powder was cycled four times in deuterium and left in the desorbed state (fifth decomposition) to produce the NaD/Al* analogue. To ensure that the majority of hydrogen atoms were replaced by deuterium, desorption was monitored by Mass Spectrometry using a Residual Gas Analyser.

In situ synchrotron radiation powder X-ray diffraction (SR-PXD) measurements were performed at the Swiss-Norwegian Beamline (SNBL, BM01A) at the European Synchrotron Radiation Facility (ESRF) in Grenoble, France. NaH/Al* powder was loaded in a single-crystal sapphire capillary (outer diameter 1.15 mm, inner diameter 0.8 mm) and mounted in a sample holder with Swagelok fittings in a glove box filled with purified argon (<1 ppm O_2 and H_2O). The sample holder was then connected to a H_2 gas filling system and the capillary heated with a hot air blower to 120 °C with a heating rate of 10 °C/min under 1 bar Ar atmosphere. While isothermal at 120 °C, 100 bar H_2 was introduced to the sample. Two-dimensional SR-PXD patterns (monochromatic X-rays with λ = 0.68291 Å) were collected during absorption using a fast pixel detector (Pilatus 2M, Dectris) with an exposure time of 26 s for a total of 6 h. The capillary was rotated 30° during exposure to improve the powder averaging. The data were integrated to one-dimensional diffraction patterns with the program Fit2D.[48]

Powder neutron diffraction (PND) experiments were conducted at ISIS Facility in England on the POLARIS instrument.[49] NaD/Al* powder was loaded into an Al high pressure sample holder inside a glove box before being attached to the "candlestick". The sample was allowed to equilibrate at 100 °C for ~30 min before addition of 100 bar D_2. Data were collected for approximately 20 mins for each the empty sample cell, sample cell containing NaD/Al* at room temperature, sample cell containing NaD/Al* at 100 °C. Upon initial addition of 100 bar D_2, data were collected for approximately 3 min per scan for a total of 15 h, after which another 20 min scan was collected.

Phase composition calculations of the data were carried out via the Rietveld fitting method using the programs GSAS[50, 51] and TOPAS Academic.[52]

Results and Discussion

In situ SR-PXD study

Data collection was initiated prior to addition of 100 bar H_2 to establish the T=0 benchmark at 100 °C. Rietveld refinement of the T=0 diffraction pattern (Fig. 1 and S2 in the Electronic Supplementary Information†) determined the composition of the crystalline phases contained in the NaH/Al* starting material to comprise of 46.5 wt% Al, 31.8 wt% NaH and 7.2 wt% NaCl, as illustrated in Fig. 2 and Table 1. The starting material was established to contain 14.4 wt% Na_3AlH_6, despite having heated this sample at 150 °C *in vacuo* for at least 24 h. Despite this, the regeneration mechanism can still be clearly observed due to the fact that $NaAlH_4$ was not detected. As anticipated, no crystalline Ti species were observed[45] nor any additional oxide impurities.

Upon addition of H_2, diffraction patterns were collected every 26 s. A 2D plot of the data collected over 6 h and a stacked plot of data collected over 1 h is illustrated in Fig. 1, where major changes in phase composition can be clearly observed. The most noticeable events are the disappearance of the NaH Bragg peaks at 2θ = 13.9 and 16.1° and the appearance of peaks at 12.9, 13.7 and 15.6° in 2θ for $NaAlH_4$, both after ca. 30 min. Although not as clear, the reflections from Al (16.7°) and Na_3AlH_6 (14.2, 14.3 and 14.4°) diminish over time but do not completely disappear. As expected, the proportion of NaCl diminishes (very slightly) between 7.2 and 6.3 wt%, throughout the experiment. NaCl is a spectator phase during the reaction. As such, it serves to measure the goodness of fit (or even an internal standard), of which to compare the phases with variable compositions. The weight percent is expected to decrease slightly as hydrogen is added into the system. The value for the weight percentage of NaCl is higher than one would expect, considering only 2 mol%, corresponding to 5.4 wt%, of $TiCl_3$ was employed as an additive. However, the exclusion

Journal Name

RSCPublishing

ARTICLE

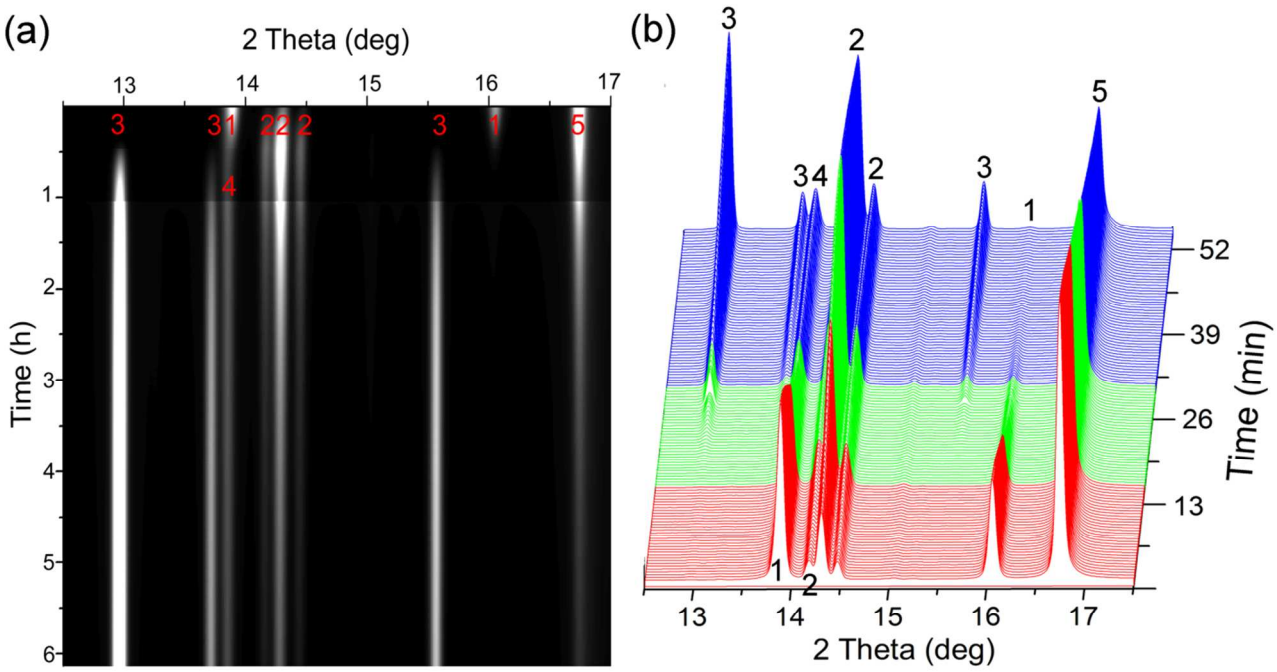

Fig. 1. (a) Two-dimensional *in situ* SR-PXD plot over 6 h and **(b)** *in situ* SR-PXD plot over 1 h of the regeneration of NaH/Al*. The Bragg peaks correspond to: 1) NaH; 2) Na_3AlH_6; 3) $NaAlH_4$; 4) NaCl; 5) Al. Red/green interface is the onset of $NaAlH_4$ formation. Green/blue interface is the maximum phase composition of Na_3AlH_5. $\lambda = 0.68291$ Å.

of amorphous phases from the calculation (particularly the Ti containing phases) renders a slight bias in the calculations.

The SR-PXD patterns collected over the first hour of hydrogenation are depicted in Fig. 1b. Within the first 20 min it is clear that the proportion of NaH and Al decreases, while Na_3AlH_6 increases. In fact, NaH is being consumed 2.6 times faster than the Al (1.16 wt%/min and 0.44 wt%/min, respectively). In terms of mol fractions, NaH is reacting 2.8 times faster than Al, which coincides with the fact that Na_3AlH_6 is the product of this reaction, requiring three atoms of Na per

Table 1 Phase composition and unit-cell dimensions measured by SR-PXD. Estimated standard deviations are given in parenthesis.

Time (min)	Al (wt%)	NaH (wt%)	Na_3AlH_6 (wt%)	$NaAlH_4$ (wt%)	NaCl (wt%)	*a*$NaAlH_4$ (Å)	*c*$NaAlH_4$ (Å)	*a*Na_3AlH_6 (Å)	*b*Na_3AlH_6 (Å)	*c*Na_3AlH_6 (Å)	*V*Na_3AlH_6 (Å^3)	*a*Al (Å)
0	46.5(1)	31.8(1)	14.4(5)	0	7.18(6)	–	–	5.4210(2)	5.5319(2)	7.7648(3)	232.851(9)	4.05970(1)
5.6	44.1(5)	26.7(6)	22.0(6)	0	7.08(5)	–	–	5.4232(2)	5.5328(2)	7.7682(2)	233.085(9)	4.05989(2)
13.4	39.5(5)	15.5(6)	38.0(6)	0.02(9)	6.98(5)	–	–	5.4267(1)	5.5357(1)	7.7723(2)	233.485(6)	4.06002(2)
19.5	38.0(5)	9.16(9)	45.4(6)	0.29(3)	7.16(5)	5.039(3)	11.44(2)	5.42776(9)	5.5367(1)	7.7737(1)	233.611(5)	4.06006(2)
30	32.2(5)	2.82(4)	50.9(5)	0.71(4)	6.95(4)	5.0387(1)	11.4323(6)	5.42895(8)	5.53739(8)	7.7754(1)	233.769(4)	4.06006(2)
52	23.4(5)	0.46(4)	39.6(5)	29.5(5)	7.02(4)	5.04019(4)	11.4354(2)	5.43004(8)	5.53908(9)	7.7771(1)	233.913(5)	4.06010(2)
120	12.3(6)	0.12(7)	19.5(9)	61.6(1)	6.56(5)	5.04065(2)	11.4370(1)	5.4305(1)	5.5393(2)	7.7775(2)	233.954(7)	4.05920(5)
180	9.8(5)	0	14.7(6)	68.8(4)	6.56(3)	5.04083(6)	11.4377(10)	5.4311(2)	5.5400(2)	7.7786(2)	234.047(9)	4.05862(7)
240	8.8 (5)	0	13.5(8)	71.2(1)	6.44(4)	5.04137(3)	11.4390(1)	5.4322(2)	5.5409(2)	7.7798(3)	234.161(1)	4.0579(1)
300	8.2(6)	0	12.5 (8)	72.8(1)	6.34(5)	5.04124(3)	11.4389(1)	5.4324(2)	5.5413(2)	7.7806(3)	234.21(1)	4.0576(1)
360	7.6(5)	0	10.7(5)	75.1(3)	6.65(4)	5.04136(3)	11.43964(10)	5.4330(2)	5.5418(2)	7.7812(3)	234.28(1)	4.0569(1)

Journal Name RSCPublishing

ARTICLE

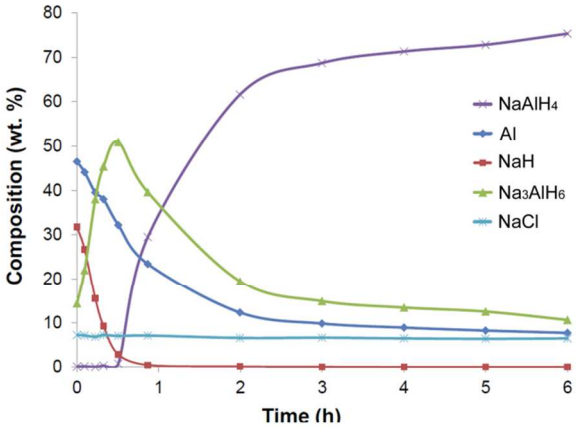

Fig. 2. Phase composition of NaH/Al* measured by SR-PXD over 6 h of hydrogenation (100 bar, 120 °C) calculated by Rietveld refinement.

Al atom (Eq. 1). The average rate of formation of Na_3AlH_6 in this time is 0.016 mol/min compared to 0.016 mol/min of Al consumed. NaH is virtually consumed within ~1 h while there is still ~22 wt% of Al remaining in the powder. During this stage of regeneration, the Al is reacting with Na_3AlH_6 to form $NaAlH_4$ thus Al is not expected to be depleted until the reaction is complete. In fact, during the 6 h of data collection the reaction rate is ~0.01 wt%/min. If all Al were to be consumed, it is estimated that an additional 13 h would be required. Previous reports concerning the hydrogenation of NaH/Al* also indicate the presence of significant quantities of Al and Na_3AlH_6 after as long as 15 h of reaction.[20, 21]

$NaAlH_4$ is observable after ~13 min, although quantification is not possible until ~20 min. The initial rate of formation is very slow and does not start to accelerate until ~30 mins at which point the rate of reaction is 1.6 wt%/min (0.03 mol/min), coinciding with maximum wt% fraction of Na_3AlH_6 (50.9 wt%). The final weight fraction of $NaAlH_4$ in the sample is 75.1 %, equivalent to 4.1 wt% H_2. This value is very comparable to previous cycling studies of $NaAlH_4$ with 2 mol% Ti additives.[53]

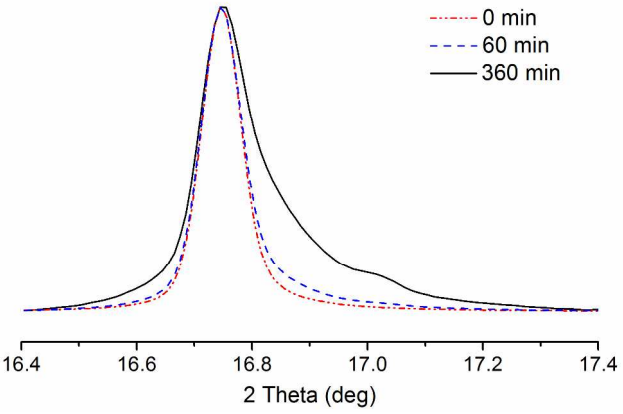

Fig. 3. Peak shape change for Al indicating formation of $Al_{1-x}Ti_x$ composites. Data normalised. λ = 0.68291 Å.

The observation that the onset of $NaAlH_4$ formation occurs before the total consumption of NaH is in agreement with the conclusions of our recent *in situ* NMR study.[20] This shows that the two reactions (Eq. 1 and 2) are not discrete. This is in contrast to the thermal decomposition of $NaAlH_4$, where NaH formation is not observed until almost all of the tetrahydride is converted to the hexahydride.[39]

During the experiment, the Bragg peak from Al at 16.75° (*hkl* = 111) becomes asymmetric (Fig. 3). Deconvolution analysis confirms that a second peak is apparent at 2θ = 16.87°. Previous *ex situ* studies of $NaAlH_4$ with Ti additives have reported this occurrence and determined this shoulder corresponds to various nanoscopic crystalline $Al_{1-x}Ti_x$ alloys.[25,26,46] A reflection at 16.87° most likely corresponds to an Al−Ti composition of c-$Al_{0.85}Ti_{0.15}$, which has often been observed for $NaAlH_4$ with $TiCl_3$ additives.[27, 44] After ~1 h of hydrogenation, a new reflection is observed at 2θ = 17.01°, which may be attributed to $Al_{1-x}Ti_x$ with $x \approx 0.20$[15] or possibly a hydrogenated c-$Ti_{0.60}Al_{0.40}H_{0.29}$ phase.[54] It is not quite possible to infer a precise composition of the alloy due to the fact that the phases typically observed always fall very close to the Al reflections in 2θ and require high resolution TEM studies to distinguish between them.[15, 22, 43, 44]

During the course of the experiment, the unit cell volume of Na_3AlH_6 increases by 0.61 % from 232.851(9) to 234.28(1) Å. This volumetric increase results from a uniform expansion of each of the Na_3AlH_6 *a*, *b* and *c* unit cell axes by 0.22, 0.18 and 0.21 %, respectively (all unit cell dimensions for Na_3AlH_6 are illustrated in Table 2). As the experiment is carried out at isothermal conditions, this behaviour was not anticipated and was not observed in previous *ex situ* experiments.[26, 55] The majority of the change occurs during the first hour, hereafter the rate of unit cell expansion decreases once $NaAlH_4$ becomes the major phase. The explanation for this phenomenon is not obvious and would require closer analysis by *in situ* XAFS or inelastic neutron scattering experiments. Ti site substitution of Al atoms may be one explanation, which has been previously predicted by first-principles density functional theory.[56] Replacement of an Al^{3+} (crystal radius 0.675 Å) with a Ti^{3+} (crystal radius 0.81 Å) would undoubtedly result in an expansion of the crystal lattice.[57] The expansion may also arise from interstitial H within the lattice. Na_3AlH_6 possesses a space

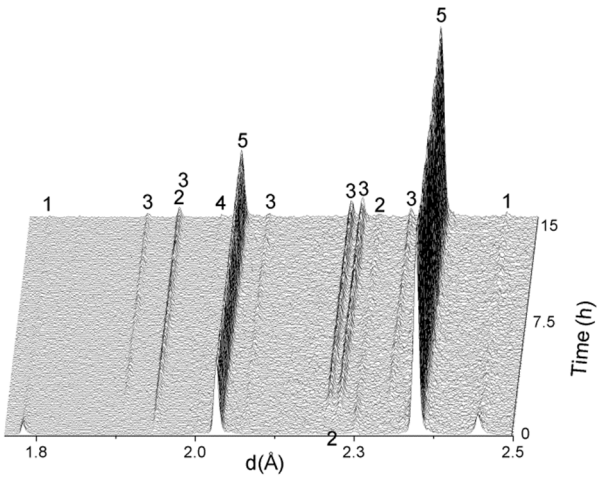

Fig. 4. *In situ* PND plot of the re generation of NaD/Al* over 15 h. The peaks correspond to: 1) NaD; 2) Na_3AlD_6; 3) $NaAlD_4$; 4) NaCl; 5) Al contained in the sample cell.

group of $P12_1/n1$ (no. 14), of which Al occupies the *2a* positions, Na the *2b* and *4e* positions, with H also occupying *4e* positions. This leaves the *2c* and *2d* sites unoccupied.[28] It has been observed previously by PXD and PND studies that site substitution does not occur for $NaAlH_4$ with Ti containing additives.[26, 28] This is corroborated in this study, as the unit cell of $NaAlH_4$ does not change during the experiment.

In situ PND study

The PND data collected on POLARIS correlate very well with the SR-PXD data. Diffraction patterns were collected every three minutes, allowing the reaction to be observed on a relatively fast time scale, with good statistics as illustrated in Fig. 4 and S3 in the Electronic Supplementary Information†. The high pressure sample cell utilised in this study was manufactured from Al, thus quantitative analysis of the Al* contained in the sample matrix was inhibited. The intense scattering of the Al sample cell also decreased the sensitivity of the technique with respect to the small quantities of some of the phases observed during the regeneration reaction. Although all of the phases identified during the SR-PXD experiment were able to be refined in this PND experiment, it is possible some minor species may have succumbed to the background.

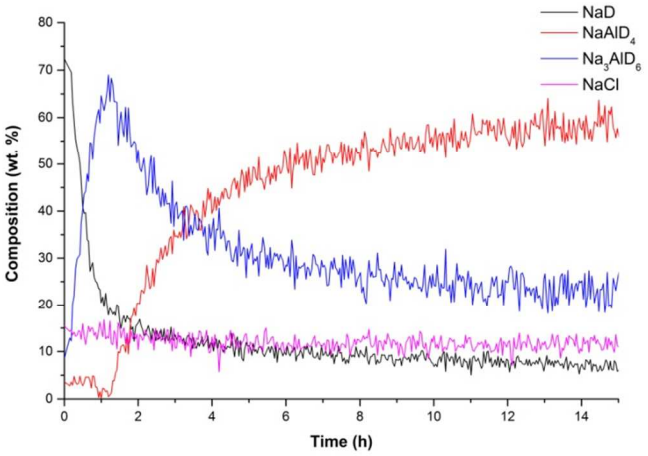

Fig. 5. Phase composition of NaD/Al* over 15 h of hydrogenation calculated by Rietveld refinement.

The PND experimental conditions were designed to be analogous to the SR-PXD and previous NMR experiments to enable direct comparison.[20] Unfortunately, the temperature rating of the sample cell would only allow for a temperature of 100 °C and the starting pressure was ~100 bar. The milder conditions inevitably slowed the rate of reaction[23] but ultimately complimented the rate of data collection and enabled the reaction to be monitored more effectively. Another factor inhibiting kinetics maybe that the sample had been cycled five times to prepare the deuterided sample.[23] Sintering of the reactant particles and sequestration of the titanium dopant in the aluminium phase may result in slower kinetics. Nevertheless, the results obtained here were very similar to those observed by the *in situ* SR-PXD experiment. Fig. 4 illustrates the changes in the diffraction patterns observed over the 15 h of reaction, while Fig. 5 depicts the wt% of each crystalline phase calculated by Rietveld refinement of the PND data (Al is not included in the refinement). Rietveld-fitted profile and difference plots for the initial NaD/Al* mixture, after 1 h of D_2 exposure and 15 h of D_2 exposure are depicted in S3 of the Electronic Supplementary Information†. The intensity of the NaD peaks are seen to diminish rapidly over time, although they do not totally disappear. Na_3AlD_6 is not observed in the initial pattern, before D_2 addition, but appears abruptly after 10 min. $NaAlD_4$ is not observed until ~1 h of reaction and coincides with the maximum wt. fraction of Na_3AlD_6. After 4 h, $NaAlD_4$ becomes the dominant phase. These results mimic those of the SR-PXD experiment albeit on an extended time scale.

The 13 min in which the $NaAlH_4$ is first observed by SR-PXD and 1 h by PND is much longer than the four minutes observed by *in situ* ^{27}Al NMR spectroscopy.[20] The primary reason is the variation in reaction conditions. Although the NMR and SR-PXD studies were carried out at 120 °C, the H_2 pressure was 100 bar for SR-PXD and 140 bar for NMR spectroscopy and previous hydrogenation studies indicate that an increase in H_2 pressure leads to an increased rate of reaction.[23] The same article also noted that temperature is the primary driving force of the reaction, with the rate increasing up to an optimal temperature of 120 °C. The reduced temperature and pressure of the PND experiment (100 °C, ~100 bars) indisputably produced a dramatic decrease in the rate of reaction. The concentration may also be below the limit of detection. NMR spectroscopy appears to have greater sensitivity and can detect the formation of $NaAlH_4$ sooner.

It is worth noting here also the difference in the data collected by powder diffraction compared with NMR spectroscopy.[20] The weight fractions indicated for the diffraction experiments only represent the fraction of polycrystalline material present. The $NaAlH_4$ signal detected after 4 min of hydrogenation may in

fact not be crystalline. If this is the case, then $NaAlH_4$ may indeed be formed earlier than indicated by Rietveld refinement of the powder diffraction data discussed here. Indeed, there are some indications that there could be formation of amorphous $NaAlH_4$ early in the reaction. In the refinements of both sets of powder diffraction data, the weight percentage of sodium chloride is constant until the formation of $NaAlH_4$ begins; thereafter it slowly decreases. This equates to an apparent increase in the molar percentage of NaCl at the beginning of the reaction. Since the NaCl is a spectator species, there is no obvious pathway by which its molar percentage should increase. Therefore, it may be possible that this indicates that some amorphous (or nanoscale) $NaAlH_4$ has been formed. This would need more careful investigation in order to confirm this hypothesis.

The observation that the onset of $NaAlH_4$ formation occurs before the total consumption of NaH both in the X-ray and neutron powder diffraction is in agreement with the conclusions of our recent *in situ* NMR study.[20] The formation of the hexahydride and tetraahydride occur concurrently, certainly to a much greater extent than in the decomposition of $NaAlH_4$.[39] In the hydrogenation reactions studied here, $NaAlH_4$ is observed after approximately 50 % of the NaH/NaD has reacted, and potentially less than that, as described above. From this observation, we can try to infer some information about the energetics of these two reactions. The fact that the decomposition reactions are essentially sequential indicates that the second reaction, the decomposition of the Na_3AlH_6 to NaH and Al (Eq. 2), has a significantly higher activation energy than the first reaction (Eq. 1). During hydrogenation, the reactions run more concurrently. Given that the enthalpy of the first hydrogenation is approximately 10 kJ/mol more exothermic than the second, it can be inferred that the difference between the two activation energies will have diminished by this amount for the hydrogenation.[58] The fact that the two reactions run concurrently indicates that the activation energy of the first hydrogenation must remain larger or approximately equal to that of the second, such that once the reaction conditions are suitable for the first hydrogenation to proceed, the other will also be favourable.

Conclusions

The *in situ* regeneration of sodium alanate has been studied by SR-PXD and PND techniques for the first time. Rietveld refinements of the data have facilitated a complete phase composition analysis, allowing the reaction pathway to be accurately determined. This study shows definitively that Al initially reacts with NaH to form Na_3AlH_6, followed by the formation of $NaAlH_4$ (before the total consumption of NaH) in two indiscrete reactions. Although this has been concluded by previous *in situ* NMR spectroscopy studies,[20] powder diffraction measurements allow the identification and quantification of all crystalline phases simultaneously whereas NMR spectroscopy is unable to do so.

Rietveld refinements of the high quality SR-PXD data depict the expansion of the Na_3AlH_6 unit cell volume throughout the experiment by 0.6 %, indicating the possibility of site substitution. The formation of crystalline $Al_{1-x}Ti_x$ phases has also been observed during the reaction, the composition of which is shown to vary over time.

Overall, this study promotes the recent development of next-generation sample holders that now enable the *in situ* diffraction measurement of hydrogen storage materials under relatively high gas pressures (>100 bar) and temperatures. The integration of next-generation fast-pixel detectors for SR-PXD and large banks of detectors for PND now enables the rapid collection of high quality data, which facilitates the study of reactions with rapid kinetics. The regeneration pathway of hydrogen storage materials is now feasible to be deduced, with quick and efficient means.

Acknowledgements

We would like to thank the project team at the Swiss Norwegian Beam Line (SNBL) at the European Synchrotron Research Facility (ESRF), Grenoble; and Dr. Ron Smith, Dr. Samantha Callear and the technical team at ISIS, Oxford. Financial assistance is acknowledged from the Research council of Norway and the Science & Technology Facilities Council, ISIS Facility.

Notes and references

[a] Physics Department, Institute for Energy Technology, P.O. Box 40, NO-2027, Kjeller, Norway. Fax: +47 63 81 09 20; Tel: +47 97 40 88 44; E-mail: bjorn.hauback@ife.no.

[b] Inorganic Chemistry Laboratory, University of Oxford, South Parks Road, Oxford, UK, OX1 3QR.

[c] ISIS Facility, Rutherford Appleton Laboratory, Chilton, Oxon, United Kingdom, OX11 0QX. Fax: +44 1235 445179; Tel: +44 1235 445179.

† Electronic Supplementary Information (ESI) available: additional information regarding the batch Rietveld refinement of PND data; Rietveld-fitted profile and difference plot for SR-PXD and PND data. See DOI: 10.1039/b000000x/

1. B. Bogdanović and M. Schwickardi, *J. Alloys Compd.*, 1997, **253**, 1-9.
2. C. M. Jensen, R. Zidan, N. Mariels, A. Hee and C. Hagen, *Int. J. Hydrogen Energy*, 1999, **24**, 461-465.
3. X. D. Kang, P. Wang, X. P. Song, X. D. Yao, G. Q. Lu and H. M. Cheng, *J. Alloys Compd.*, 2006, **424**, 365-369.
4. Z. Dehouche, L. Lafi, N. Grimard, J. Goyette and R. Chahine, *Nanotechnology*, 2005, **16**, 402-409.
5. Y. Suffisawat, P. Rangsunvigit, B. Kitiyanan, N. Muangsin and S. Kulprathipanja, *Int. J. Hydrogen Energy*, 2007, **32**, 1277-1285.
6. X. Z. Xiao, L. X. Chen, X. H. Wang, S. Q. Li, Z. M. Hang, C. P. Chen and Q. D. Wang, *Phys. Scr.*, 2007, **T129**, 95-98.
7. P. Wang, X. D. Kang and H. M. Cheng, *J. Alloys Compd.*, 2006, **421**, 217-222.
8. C. M. Jensen and K. J. Gross, *Appl. Phys. A: Mater. Sci. Process.*, 2001, **72**, 213-219.
9. G. Sandrock, K. Gross and G. Thomas, *J. Alloys Compd.*, 2002, **339**, 299-308.
10. R. A. Zidan, S. Takara, A. G. Hee and C. M. Jensen, *J. Alloys Compd.*, 1999, **285**, 119-122.
11. P. Wang and C. M. Jensen, *J. Phys. Chem. B*, 2004, **108**, 15827-15829.

12. T. Wang, J. Wang, A. D. Ebner and J. A. Ritter, *J. Alloys Compd.*, 2008, **450**, 293-300.
13. Y. Suttisawat, V. Jannatisin, P. Rangsunvigit, B. Kitiyanan, N. Muangsin and S. Kulprathipanja, *J. Power Sources*, 2007, **163**, 997-1002.
14. C. P. Balde, H. A. Stil, A. M. J. van der Eerden, K. P. de Jong and J. H. Bitter, *J. Phys. Chem. C*, 2007, **111**, 2797-2802.
15. M. P. Pitt, P. E. Vullum, M. H. Sørby, H. Emerich, M. Paskevicius, C. E. Buckley, E. M. Gray, J. C. Walmsley, R. Holmestad and B. C. Hauback, *J. Alloys Compd.*, 2012, **521**, 112-120.
16. K. J. Gross, G. Sandrock and G. J. Thomas, *J. Alloys Compd.*, 2002, **330**, 691-695.
17. R. Cantelli, O. Palumbo, A. Paolone, C. M. Jensen, M. T. Kuba and R. Ayabe, *J. Alloys Compd.*, 2007, **446**, 260-263.
18. P. Wang, X. D. Kang and H. M. Cheng, *J. Phys. Chem. B*, 2005, **109**, 20131-20136.
19. S. D. Beattie and G. S. McGrady, *Int. J. Hydrogen Energy*, 2009, **34**, 9151-9156.
20. T. D. Humphries, D. Birkmire, B. C. Hauback, G. S. McGrady and C. M. Jensen, *Phys. Chem. Chem. Phys.*, 2013, **15**, 6179-6181.
21. B. Bogdanović, M. Felderhoff, M. Germann, M. Hartel, A. Pommerin, F. Schuth, C. Weidenthaler and B. Zibrowius, *J. Alloys Compd.*, 2003, **350**, 246-255.
22. M. P. Pitt, P. E. Vullum, M. H. Sørby, D. Blanchard, M. P. Sulic, H. Emerich, M. Paskevicius, C. E. Buckley, J. Walmsley, R. Holmestad and B. C. Hauback, *J. Alloys Compd.*, 2012, **513**, 597-605.
23. D. L. Sun, S. S. Srinivasan, G. R. Chen and C. M. Jensen, *J. Alloys Compd.*, 2004, **373**, 265-269.
24. K. Bai and P. Wu, *Appl. Phys. Lett.*, 2006, **89**.
25. S. Isobe, H. Yao, Y. Wang, H. Kawasaki, N. Hashimoto and S. Ohnuki, *Int. J. Hydrogen Energy*, 2010, **35**, 7563-7567.
26. H. W. Brinks, C. M. Jensen, S. S. Srinivasan, B. C. Hauback, D. Blanchard and K. Murphy, *J. Alloys Compd.*, 2004, **376**, 215-221.
27. H. W. Brinks, B. C. Hauback, S. S. Srinivasan and C. M. Jensen, *J. Phys. Chem. B*, 2005, **109**, 15780-15785.
28. P. Canton, M. Fichtner, C. Frommen and A. Leon, *J. Phys. Chem. B*, 2006, **110**, 3051-3054.
29. J. Graetz, J. J. Reilly, J. Johnson, A. Y. Ignatov and T. A. Tyson, *Appl. Phys. Lett.*, 2004, **85**, 500-502.
30. S. I. Orimo, Y. Nakamori, J. R. Eliseo, A. Zuttel and C. M. Jensen, *Chem. Rev.*, 2007, **107**, 4111-4132.
31. A. Zuttel, *Naturwissenschaften*, 2004, **91**, 157-172.
32. H. W. Li, Y. G. Yan, S. Orimo, A. Zuttel and C. M. Jensen, *Energies*, 2011, **4**, 185-214.
33. T. D. Humphries, D. Birkmire, B. C. Hauback, G. S. McGrady and C. M. Jensen, *J. Mater. Chem. A*, 2013, **1**, 2974-2977.
34. T. D. Humphries, G. N. Kalantzopoulos, I. Llamas-Jansa, J. E. Olsen and B. C. Hauback, *J. Phys. Chem. C*, 2013, **117**, 6060-6065.
35. S. Satyapal, J. Petrovic and G. Thomas, *Sci. Am.*, 2007, **296**, 80-87.
36. M. Ismail, Y. Zhao, X. B. Yu, J. F. Mao and S. X. Dou, *Int. J. Hydrogen Energy*, 2011, **36**, 9045-9050.
37. C. Pistidda, S. Garroni, C. B. Minella, F. Dolci, T. R. Jensen, P. Nolis, U. Boeenberg, Y. Cerenius, W. Lohstroh, M. Fichtner, M. D. Baro, R. Bormann and M. Dornheim, *J. Phys. Chem. C*, 2010, **114**, 21816-21823.
38. C. Pistidda, E. Napolitano, D. Pottmaier, M. Dornheim, T. Klassen, M. Baricco and S. Enzo, *Int. J. Hydrogen Energy*, 2013, **38**, 10479-10484.
39. K. J. Gross, S. Guthrie, S. Takara and G. Thomas, *J. Alloys Compd.*, 2000, **297**, 270-281.
40. P. E. Vullum, M. P. Pitt, J. C. Walmsley, B. C. Hauback and R. Holmestad, *J. Alloys Compd.*, 2011, **509**, 281-289.
41. G. Majer, E. Stanik, B. L. E. Valiente, F. Grinberg, O. Kircher and M. Fichtner, *J. Alloys Compd.*, 2005, **404-406**, 738-742.
42. E. C. Ashby and P. Kobetz, *Inorg. Chem.*, 1966, **5**, 1615-1617.
43. M. Felderhoff, K. Klementiev, W. Grunert, B. Spliethoff, B. Tesche, J. M. Bellosta von Colbe, B. Bogdanovic, M. Hartel, A. Pommerin, F. Schuth and C. Weidenthaler, *Phys. Chem. Chem. Phys.*, 2004, **6**, 4369-4374.
44. M. P. Pitt, P. E. Vullum, M. H. Sørby, H. Emerich, M. Paskevicius, C. E. Buckley, E. M. Gray, J. C. Walmsley, R. Holmestad and B. C. Hauback, *Philos. Mag.*, 2013, **93**, 1080-1094.
45. A. G. Haiduc, H. A. Stil, M. A. Schwarz, P. Paulus and J. J. C. Geerlings, *J. Alloys Compd.*, 2005, **393**, 252-263.
46. C. Weidenthaler, A. Pommerin, M. Felderhoff, B. Bogdanovic and F. Schuth, *Phys. Chem. Chem. Phys.*, 2003, **5**, 5149-5153.
47. A. Léon, O. Kircher, H. Rösner, B. Décamps, E. Leroy, M. Fichtner and A. Percheron-Guégan, *J. Alloys Compd.*, 2006, **414**, 190-203.
48. A. P. Hammersley, *Fit2D: An introduction and Overview; ESRF Internal Report.*, 1997,
49. S. Hull, R. I. Smith, W. I. F. David, A. C. Hannon, J. Mayers and R. Cywinski, *Physica B*, 1992, **180-181**, 1000-1002.
50. B. H. Toby, *J. Appl. Crystallogr.*, 2001, **34**, 210-213.
51. A. C. Larson and R. B. Von Dreele, *Los Alamos National Laboratory Report LAUR*, 2000, 86-748.
52. TOPAS-Academic, http://www.topas-academic.net/, Accessed May 2014.
53. S. S. Srinivasan, H. W. Brinks, B. C. Hauback, D. L. Sun and C. M. Jensen, *J. Alloys Compd.*, 2004, **377**, 283-289.
54. K. Hashi, K. Ishikawa, K. Suzuki and K. Aoki, *J. Alloys Compd.*, 2002, **330-332**, 547-550.
55. K. Sakaki, Y. Nakamura, E. Akiba, M. T. Kuba and C. M. Jensen, *J. Phys. Chem. C*, 2010, **114**, 6869-6873.
56. K. J. Michel and V. Ozolins, *J. Phys. Chem. C*, 2011, **115**, 21454-21464.
57. R. D. Shannon, *Acta Crystallogr A*, 1976, **32**, 751-767.
58. R. H. Jones and G. J. Thomas, *Materials for the hydrogen economy*, CRC Press, Boca Raton, 2008, 191-209.

The regeneration pathway of sodium alanate has been studied by *in situ* synchrotron powder X-ray diffraction and powder neutron diffraction.